Nonlinear Stress Relaxation of ABS Polymers in the Molten State

Yuji Aoki* and Akira Hatano

Chemical Science Laboratories, Mitsubishi Chemical Corporation, 1, Toho-cho, Yokkaichi, Mie 510-8530, Japan

Takeshi Tanaka

ACT Research Center Inc., 3-3-7, Obata, Yokkaichi, Mie 510-0875, Japan

Hiroshi Watanabe*

Institute for Chemical Research, Kyoto University, Uji, Kyoto 611-0011, Japan

Received December 6, 2000; Revised Manuscript Received February 7, 2001

ABSTRACT: Large deformation, nonlinear stress relaxation behavior was examined in the molten state for two types of ABS polymers, with one type containing well-dispersed rubber particles and the other, agglomerated rubber particles. These different morphologies were accomplished by adjusting the chemical composition of poly(styrene-*co*-acrylonitrile) (SAN) grafted on the rubber particles, such that the acrylonitrile content of the grafted SAN is equal to or different from that of the matrix SAN. The time-strain separability was found for the nonlinear relaxation of the matrix/grafted SAN chains in those ABS polymers. In the ABS polymer containing randomly dispersed rubber particles, the damping function $h(\gamma)$ of the SAN chains was more strongly dependent on the strain γ than $h(\gamma)$ of the pure matrix SAN chains. This difference was attributed to the filler effect in that ABS polymer. In contrast, in the ABS polymers containing networks of the agglomerated rubber particles, the SAN chains exhibited less γ-dependent $h(\gamma)$ that is close to the pure matrix chains, possibly due to lack of the filler effect in large pockets formed in this network.

Introduction

Acrylonitrile−butadiene−styrene (ABS) polymer is one of the most typical two-phase polymers and consists of a continuous poly(styrene-*co*-acrylonitrile (SAN) phase in which the rubber phase (polybutadiene grafted with SAN) is dispersed in the form of spherical particles. In general, ABS polymer is made by graft copolymerization of styrene and acrylonitrile monomers in the presence of rubber latices by emulsion polymerization. During the polymerization, some of SAN chains are grafted on the rubber particles. These grafted SANs are believed to act as a dispersing agent due to the repulsive force between the grafted polymers.

For about two decades, we have been investigating the linear viscoelastic properties of several kinds of molten ABS polymers composed of SAN-grafted rubber particles and molten SAN matrix.[1−8] We found that there are two kinds of ABS polymers exhibiting different dynamic viscoelastic behavior. One was the ABS polymer with the rubber particles being agglomerated in the matrix SAN phase, and the other was the ABS containing finely dispersed particles.[1,2] The viscoelastic properties of ABS polymers were influenced by the AN content, w_{AN}, in the grafted SAN.[3] When the difference in w_{AN} between the grafted and matrix SAN was small, the rubber particles were dispersed finely without agglomeration. The mismatching of w_{AN} caused the agglomeration of rubber particles and led to emergence of the very slow relaxation associated with the so-called second plateau in the storage modulus.

We also investigated the effect of grafting degree g_d (mass of grafted SAN/mass of rubber particles) on the viscoelastic properties for ABS polymers.[7,8] At low frequencies (ω) where the molecular relaxation of individual matrix/graft SAN chains is completed, the storage modulus (G') and loss modulus (G'') first decreased and then increased with increasing g_d. The rubber particles in the ABS samples showing the minimum G' and G'' values at such low ω and a given temperature were finely dispersed, but the particles in the other samples exhibiting the second plateau formed an agglomerated structure or three-dimensional network structure. This minimum occurred at $g_d \cong 0.4$ and 0.2 for the ABS polymers having rubber particle size of 170 and 350 nm, respectively.

The ABS polymers having these g_d values exhibited only weak slow relaxation modes and no clear second plateau in G' because of the lack of strong agglomerates therein, and the increase of the moduli with either increasing or decreasing g_d from those values resulted from enhanced agglomeration. The above facts show that there is an optimum graft density σ (number of grafted SAN chains/unit surface area of rubber particles) for dispersing the rubber particles. Hasegawa et al.[8] calculated the interaction free energy between two grafted polymer plates in polymer melt using a mean field approximation. They found that the interaction has an attractive part and that the depth of this part varies with σ. The optimum σ value, giving the least depth of the attraction, was found to be independent of the particle diameter. Thus, a good dispersion of rubber particles requires the optimum graft density[7,8] as well as the matching of the AN content between the matrix and grafted SANs.[3]

In addition to the linear viscoelasticity explained above, nonlinear viscoelasticity of ABS polymer is important for its melt processing such as extrusion, injection, thermoforming, and blow molding. In the processing, the polymer melts often undergo extreme

* To whom correspondence should be addressed.

10.1021/ma002076l CCC: $20.00
Published on Web 03/23/2001

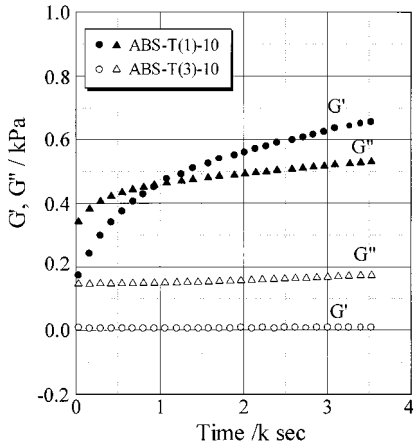

Figure 1. Time sweep at 240 °C and $\omega = 0.04$ rad s^{-1} for the ABS-T(1)-10 and ABS-T(3)-10.

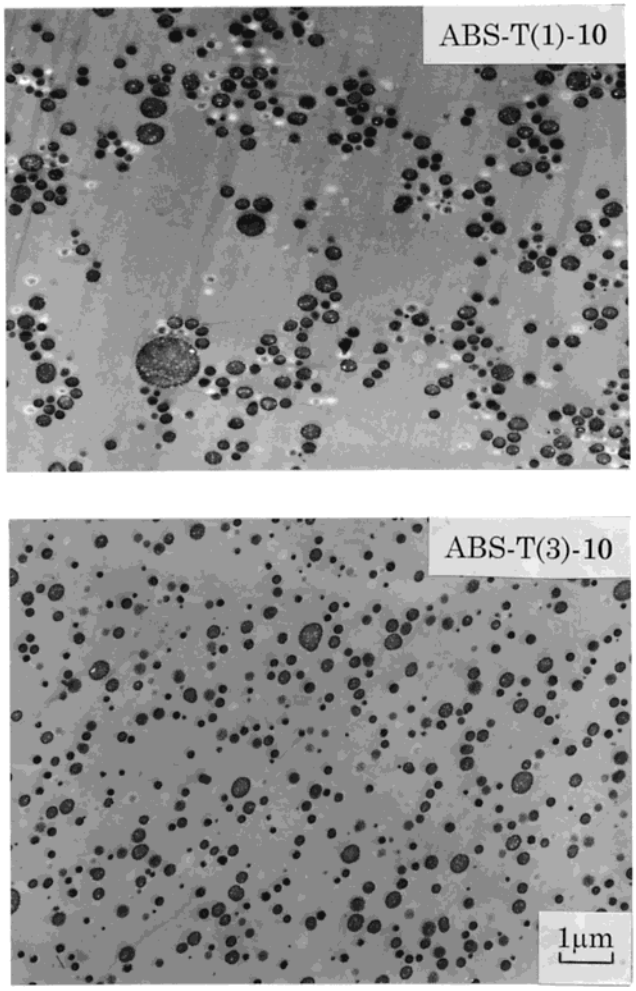

Figure 2. Electron micrographs of ABS-T(1)-10 (a) and ABS-T(3)-10 (b) after annealing at 240 °C for 1 h.

strains at high strain rates. Large deformation shear relaxation modulus $G(t,\gamma)$, where t is a time and γ is a shear strain, is one of the most important nonlinear viscoelastic quantities.

In general, $G(t,\gamma)$ of entangled *homopolymers* can be expressed by

$$G(t,\gamma) = G(t)\, h(\gamma) \quad \text{at long } t \tag{1}$$

where $G(t)$ is the linear relaxation modulus and $h(\gamma)$ is the damping function.[9] This time-strain separability is

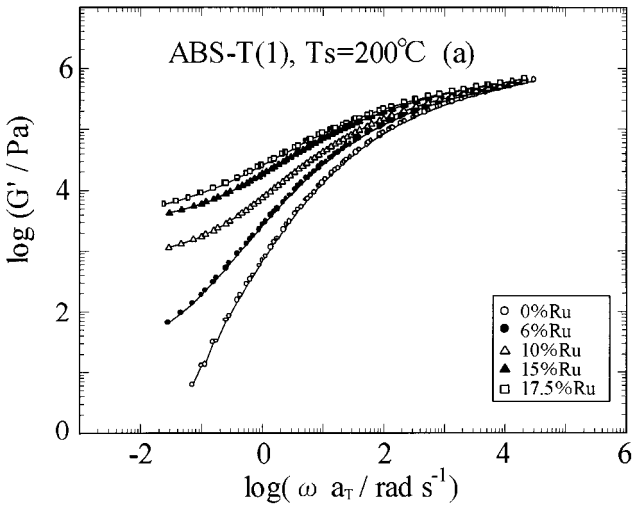

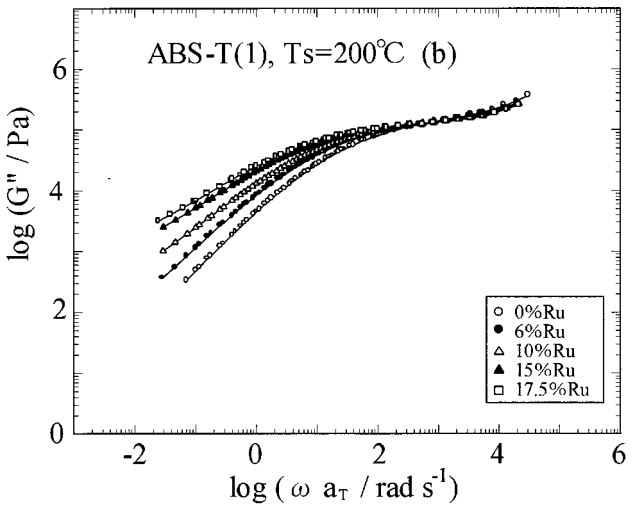

Figure 3. Master curves of the storage modulus G' (a) and the loss modulus G'' (b) for ABS-T(1) at 200 °C.

consistent with the Bernstein−Kearlsley−Zapas (BKZ) constitutive model although the separability itself is not uniquely related to this constitutive equation.[10] For respective materials of our interest, we would like to examine the time-strain separability and the damping function, as there are many types of the damping functions of polymer melts according to the molecular weight distribution and branching.[9] This is the case not only for homopolymers but also for our ABS polymers.

Partly from this point of view, Takahashi et al.[11] studied nonlinear viscoelasticity of ABS polymers having well-dispersed rubber particles. The ABS polymers exhibited fast and slow relaxation processes attributable to the motion of matrix/graft SAN chains and rubber particles, respectively. Takahashi et al. reported that $G(t,\gamma)$ for the fast process exhibited nonlinear decreases with increasing γ and this nonlinearity disappeared for $G(t,\gamma)$ for the slow process. However, they rather focused their attention on the slow process and did not fully examine the details of the nonlinearity for the fast relaxation, e,g., validity of the time-strain separability.

In this paper, we focus our attention on this nonlinearity of the fast relaxation of the matrix/graft SAN chains. For this purpose, we prepared two different types of ABS polymers with various rubber contents. One type contained the network structure of rubber particles, and the other, well-dispersed rubber particles.

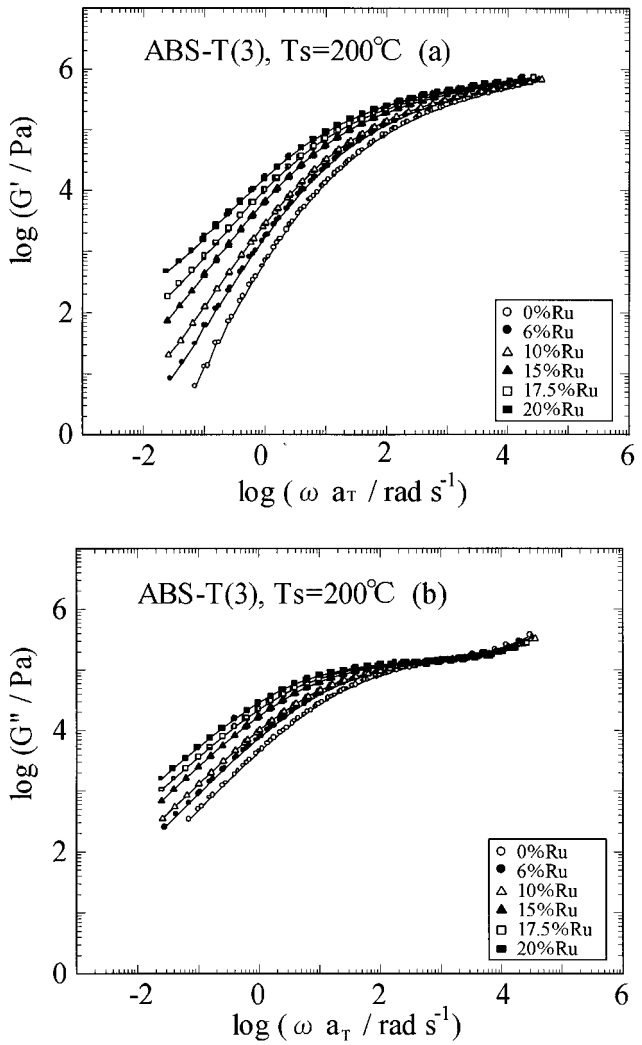

Figure 4. Master curves of the storage modulus G' (a) and the loss modulus G'' (b) for ABS-T(3) at 200 °C.

We measured the linear viscoelastic moduli and nonlinear $G(t,\gamma)$ of the ABS samples and examined the time-strain separability of the $G(t,\gamma)$ in the range of t where the SAN chains relaxed. This paper presents the results and discusses the effect of the state of dispersion of the rubber particles on the damping function of the SAN chains in ABS polymer.

Experimental Section

Materials. Two series of ABS polymers (ABS-T(1) and ABS-T(3)) with various rubber contents w_r were used in this work. ABS-T(1) and ABS-T(3) were made from the same polybutadiene particle and the same matrix SAN. The particle diameter in the ABS polymers was about 300 nm, and the grafting degree, defined as the weight ratio of grafted SAN to rubber (polybutadiene) particles, was about 1.00 for both series. These grafting degrees are pretty large, because these ABS polymers include many occluded SAN besides grafted SAN. The rubber content is $w_r = 0$ (SAN), 6, 10, 15, 17.5, and 20 wt %.

The matrix SAN (SAN-29) sample was prepared by radical polymerization. Its weight-average molecular weight (M_w) and polydispersity index (M_w/M_n) were 7.7×10^4 and 2.6, respectively, and the AN content $w_{AN} = 29.2$ wt %. (These M_w, M_w/M_n, and w_{AN} values were determined with light scattering (Otsuka Electronics, DLS-700), GPC (Waters, ALC/GPC model 150C), and elementary analysis (Yanaco, CHN coder), respectively.)

The only difference between the ABS-T(1) and ABS-T(3) samples was the w_{AN} of the grafted SAN, ~24 wt % for ABS-T(1) and ~29 wt % for ABS-T(3). Thus, the mismatching of w_{AN} of the matrix and grafted SAN in ABS-T(1) resulted in agglomeration of the rubber particles, while no agglomeration occurred in the matched ABS-T(3). Hereafter, the ABS polymers are designated by a code ABS-T(x)-w_r, where x (= 1 or 3) indicates the type of ABS and w_r the rubber particle content (in wt %).

Viscoelastic Measurements. Dynamic viscoelastic and step-shear stress relaxation measurements were carried out with a Rheometric ARES-2KFRTN1. A parallel-plates geometry with 25 mm diameter and a cone-plate geometry with a gap angle of 0.0845 rad and 25 mm diameter were used in dynamic and stress relaxation modes, respectively. In the stress relaxation experiments, the shear strain ranged from 0.01 to 4.5. In the dynamic measurements, the storage modulus (G') and loss modulus (G'') were obtained as a function of angular frequency (ω). The G' and G'' were measured at different temperatures in order to investigate the temperature dependence of the viscoelastic properties. The time−temperature superposition[12] was applicable, and the G' and G'' data were superimposed onto the master curves at 200 °C. All measurements were performed under nitrogen so as to minimize oxidative degradation at high temperatures.

Results and Discussion

Time Sweep Experiments for ABS-T(1) and ABS-T(3). We conducted time sweeps of G' and G'' at 240 °C and $\omega = 0.04$ rad/s for the *as-prepared* samples of ABS-T(1)-10 and ABS-T(3)-10. The results are shown in Figure 1. A great increase of G' and G'' with time is observed for ABS-T(1)-10, but not for ABS-T(3)-10. This result indicates that the dispersion state of rubber particles at high temperature was unstable for ABS-T(1) but stable for ABS-T(3). Electron microscopic observation indicated that there were no differences in morphology between as-prepared ABS-T(1) and ABS-T(3), and both had well-dispersed particles. However, agglomeration of rubber particles was detected for ABS-T(1) and not for ABS-T(3) after the time sweep experiments at 240 °C, as shown in Figure 2a,b.

Thus, ABS-T(1) forms the network structure of the rubber particles on annealing at the high temperature 240 °C (because of the mismatching of w_{AN} in the matrix and grafted SAN chains). To examine the viscoelastic properties of the well-stabilized network, we annealed ABS-T(1) samples at 240 °C for 1 h prior to the viscoelastic tests. After this annealing treatment, the network structure was stabilized at lower temperatures $T \leq 220$ °C, and its viscoelastic behavior was examined in this range of T.

The as-prepared ABS-T(3) samples were stable at $T \leq 220$ °C without the annealing at 240 °C (cf. Figures 1 and 2). Thus, we measured the viscoelastic properties of these as-prepared samples without annealing.

Linear Viscoelastic Behavior of ABS Polymers. The G' and G'' vs ω curves at various T were excellently superimposed into a master curve by shifts along the ω axis by a factor a_T. Figures 3 and 4 respectively show the master curves for ABS-T(1) and ABS-T(3) with various rubber contents at 200 °C. The T dependence of the shift factor a_T was almost the same irrespective of rubber content. As similar to the behavior of previously examined ABS polymers,[1] the a_T of the ABS-T(1) and ABS-T(3) were well described by the WLF equation[12] with constant coefficients c_1 (=8.86) and c_2 (=101.6),

$$\log a_T = -c_1(T - T_s)/(c_2 + T - T_s) \qquad (2)$$

Provided that data are taken over a sufficiently wide

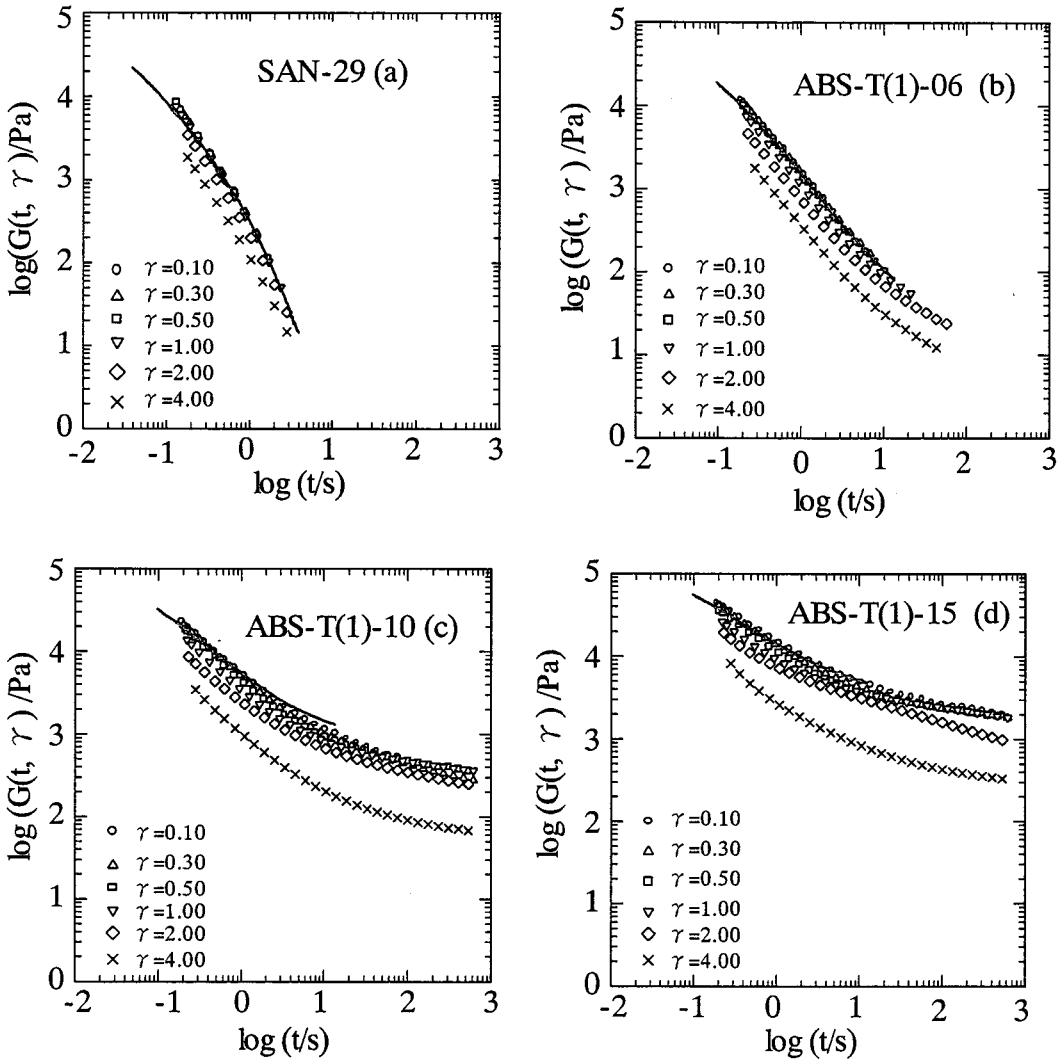

Figure 5. Stress relaxation modulus $G(t,\gamma)$ at various strains γ obtained for SAN-29 and ABS-T(1) at 200 °C. The solid curves indicate the linear relaxation modulus calculated from the G' and G'' data.

temperature range, the reference temperature T_s (for these c_1 and c_2) can be determined within ±1 °C. For the ABS-T(1) and ABS-T(3) polymers, T_s was 137 ± 1 °C.

As seen in Figures 3 and 4, the rubbery plateau modulus (estimated as the G' value at $\omega \cong 10^4$ rad s^{-1} where G'' begins to increase significantly because of the rubber-to-glass transition) does not depend much on the rubber particle content w_r, because of the similarity in the rigidity of these particle and matrix SAN in the rubbery plateau region.[5] This plateau extends to the lower ω with increasing w_r, suggesting that the relaxation of the matrix/graft SAN becomes slower due to the presence of the rubber particles. In the rubbery plateau region, we cannot find the difference between ABS-T(1) and ABS-T(3) having the same rubber content.

The most remarkable viscoelastic features of the ABS polymers are seen at lower ω. At $\omega = 1-100$ rad s^{-1}, both ABS-T(1) and ABS-T(3) exhibit the relaxation following the rubbery plateau. This relaxation is attributable to motion of the matrix/graft SAN chains being retarded with increasing w_r. This increase results from enhanced entanglements between the grafted SAN chains, thereby retarding the relaxation of these chains. This retardation for the grafted SAN chains further leads to an increase of a lifetime of the entanglements between the grafted and matrix SAN chains and thus to the retarded relaxation of the matrix chains as well.

The above relaxation of the matrix/graft SAN chains is not too much different for the ABS-T(1) and ABS-T(3), the former containing agglomerated network of the rubber particles while the latter, well-dispersed particles. However, a difference between these ABS's becomes prominent at $\omega < 1$ rad s^{-1} where the relaxation of the SAN chains is almost completed. For the ABS-T(1) (Figure 3), G' tends to level off to exhibit the so-called "second plateau" with decreasing $\omega < 1$ rad s^{-1}. This plateau corresponds to an initial modulus for a very slow relaxation of the agglomerated network. (This relaxation itself is too slow to be detected in our experimental window.) The second plateau becomes more prominent with increasing w_r.

In contrast, the ABS-T(3) (Figure 4) does not clearly exhibit the second plateau even at the highest rubber content (20%). However, the lack of the terminal behavior of G' ($\propto\omega^2$) noted in Figure 4a demonstrates that the terminal relaxation of the ABS-T(3) is slower than the SAN chain relaxation. This terminal relaxation (again too slow to be detected in our experimental window) can be attributed to motion of well-dispersed rubber particles.

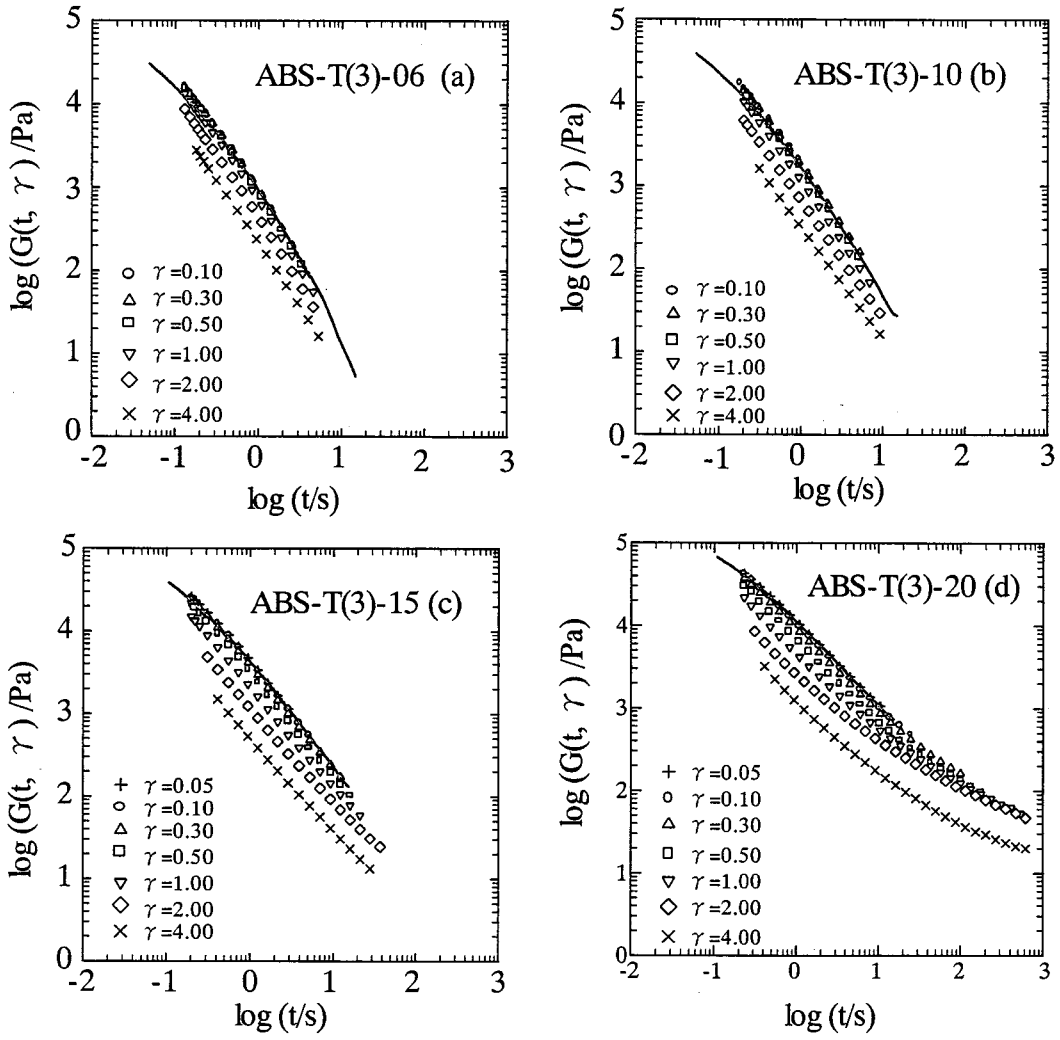

Figure 6. Stress relaxation modulus $G(t,\gamma)$ at various strains γ obtained for ABS-T(3) at 200 °C. The solid curves indicate the linear relaxation modulus calculated from the G' and G'' data.

Nonlinear Relaxation Modulus $G(t,\gamma)$ of ABS Polymers. Figure 5a−d shows the nonlinear relaxation modulus $G(t,\gamma)$ of SAN-29 and ABS-T(1), and Figure 6a−d, $G(t,\gamma)$ of ABS-T(3), both at 200 °C. To confirm the linearity for small γ, we also present the linear relaxation modulus $G(t)$ calculated from the G' and G'' data. The solid curves represent this $G(t)$ obtained with the method of Ninomiya and Ferry.[12]

$$G(t) = [G'(\omega) - 0.4G''(0.4\omega) + 0.014G''(10\omega)]_{\omega=1/t} \quad (3)$$

For the pure matrix SAN-29 (Figure 5a), the $G(t,\gamma)$ curves for $\gamma \leq 0.5$ are very close to each other and agree with the linear $G(t)$ curve. This $G(t,\gamma)$ decreases with increasing $\gamma > 0.5$, and the nonlinearity prevails.

As seen in Figures 5 and 6, the relaxation of $G(t,\gamma)$ of both ABS-T(1) and ABS-T(3) is slower than that of the matrix SAN-29 because of the mechanisms explained earlier for the linear viscoelastic behavior. More importantly, the $G(t,\gamma)$ of these ABS's exhibit pronounced damping at large γ. For these $G(t,\gamma)$ data, validity of the time-strain separability (eq 1) is examined below.

In Figures 7 and 8, the $G(t,\gamma)$ curves of ABS-T(1) and ABS-T(3), respectively, are shifted vertically (in the double-logarithmic scales) to be superposed on respective reference curves obtained for the smallest γ (= 0.1 or 0.05). These reference curves are in agreement with the linear $G(t)$ curves. In the entire range of t examined, good superposition is achieved for ABS-T(1) and ABS-T(3) having small rubber content. Thus, in that range, the time-strain separability is valid for these ABS's.

However, the superposition becomes poorer with increasing rubber content w_r for both ABS's, in particular for the ABS-T(3)-20 (Figure 8d). This failure of superposition can be attributed to a fact that the $G(t,\gamma)$ data in the range of t examined are contributed from different relaxation mechanisms explained earlier, i.e., the mechanisms for the matrix/graft SAN chains, agglomerated networks (in the ABS-T(1)), and the well-dispersed rubber particles (ABS-T(3)). The magnitude of damping should be different for these mechanisms. (In fact, Takahashi et al.[11] found that the last mechanism is associated with the damping much weaker than that of polymeric relaxation.) For large w_r, those mechanisms comparably contribute to the $G(t,\gamma)$ data, thereby resulting in the failure of the superposition. In relation to this argument, the success of the superposition for small w_r is attributed to minor contributions from the relaxation mechanisms for the agglomerates/rubber particles.

Our main interest in this paper is placed on the nonlinear damping behavior of the matrix/graft SAN chains. This behavior is best examined if we could subtract the contributions from the agglomerates/rubber particles relaxation (in a way similar to that utilized

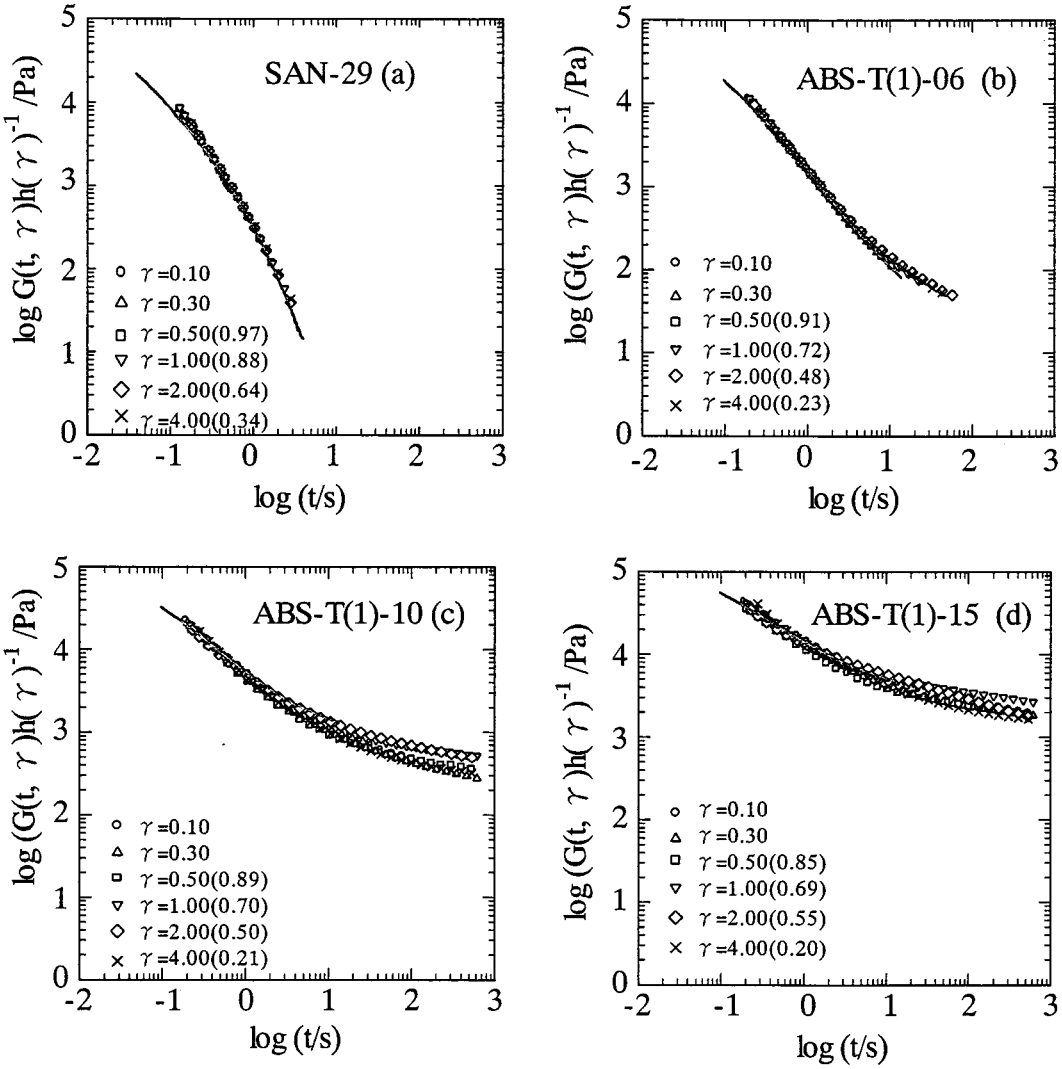

Figure 7. Plots of $G(t,\gamma)/h(\gamma)$ against time for SAN-29 and ABS-T(1) at 200 °C.

for block copolymer micellar systems[13] for which the terminal relaxation was detected). However, our ABS's do not fully relax in our experimental window (cf. Figures 3−6), and this subtraction cannot be accurately achieved. Thus, in this paper, we evaluate the damping function for the SAN chain relaxation process as

$$h(\gamma) = [G(t,\gamma)/G(t)]_{t=1\text{s}} \tag{4}$$

At the reference time utilized in eq 4, $t = 1$ s, the SAN chain relaxation is close to completion, and the slower relaxation of the agglomerates/rubber particles hardly begins, as judged from the inflection of the G' curves seen at $\omega \cong 1\ \text{s}^{-1}$ (cf. Figures 3 and 4). Thus, from our $G(t,\gamma)$ data, the damping of the SAN chains is most appropriately quantified with the $h(\gamma)$ defined by eq 4. In fact, in Figures 7 and 8, the $G(t,\gamma)$ data reduced by this $h(\gamma)$ exhibit satisfactory superposition at $t \leq 1$ s even for the largest particle content, indicating the validity of the time-strain separability for the SAN chain relaxation. The $h(\gamma)$ data thus obtained for ABS-T(3) and ABS-T(1) are discussed below in relation to the molecular origin of the damping.

Damping Function of ABS-T(3). Figure 9 illustrates the damping function $h(\gamma)$ of the SAN chains in ABS-T(3) with various rubber contents w_r. For comparison, $h_{\text{SAN}}(\gamma)$ of the pure matrix SAN-29 ($M_w/M_n = 2.6$) is also shown. These $h_{\text{SAN}}(\gamma)$ data are close to $h(\gamma)$ of a polystyrene (PS) having a similarly broad molecular weight distribution ($M_w/M_n = 2.5$).[14] The damping of these entangled SAN-29 and PS chains is commonly attributed to the chain shrinkage occurring faster than the orientational relaxation (chain rotation) after step strain.[15]

As seen in Figure 9, the damping of the matrix/graft SAN chains in ABS-T(3) becomes stronger with increasing w_r. This strong damping is expected to be still related to the mechanism characteristic of the entangled chains, i.e., the chain shrinkage faster than rotation, and the only difference between the SAN chains in ABS-T(3) (having well-dispersed rubber particles) and the pure matrix SAN-29 chains would be a local strain γ_{local} for the former chains that is enhanced by the filler effect:[16] In the time scale ($t = 1$ s) where we have evaluated the $h(\gamma)$ data, the rubber particles are much stiffer than the SAN chains and can effectively work as the fillers.

To examine this expectation, we evaluated γ_{local} for the case of the simplest filler effect,[5,16]

$$\gamma_{\text{local}} = [1 + 2.5\phi + 14.1\phi^2]\gamma \tag{5}$$

where γ is the externally applied (nominal) strain, and ϕ ($\propto w_r$) is the volume fraction of the rubber particles

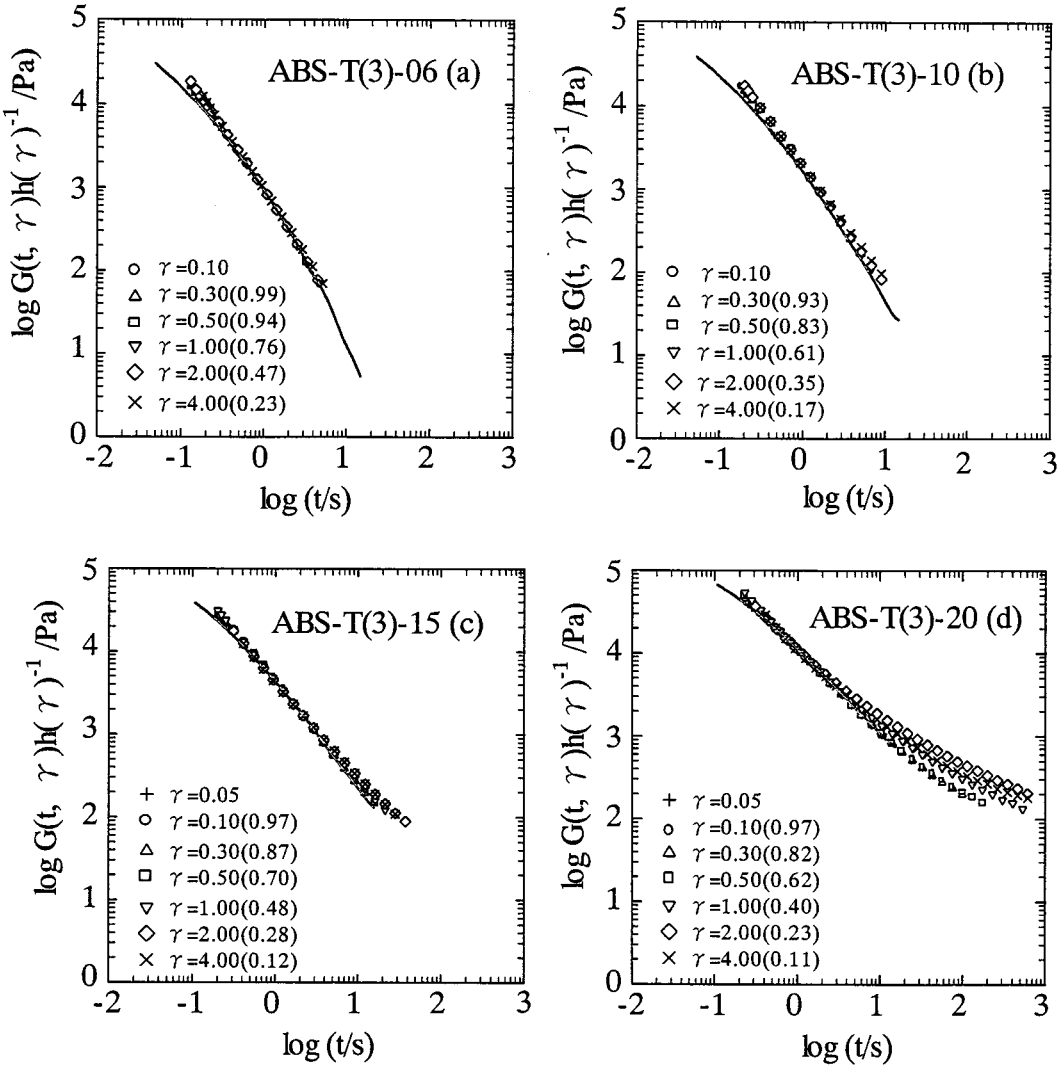

Figure 8. Plots of $G(t,\gamma)/h(\gamma)$ against time for ABS-T(3) at 200 °C.

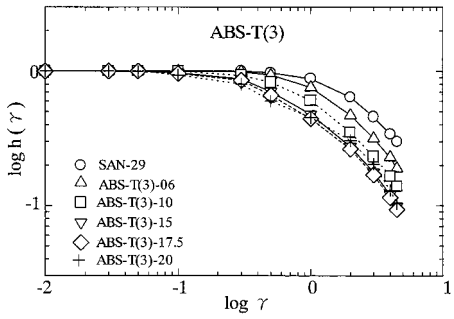

Figure 9. Damping functions $h(\gamma)$ of ABS-T(3) having different rubber content.

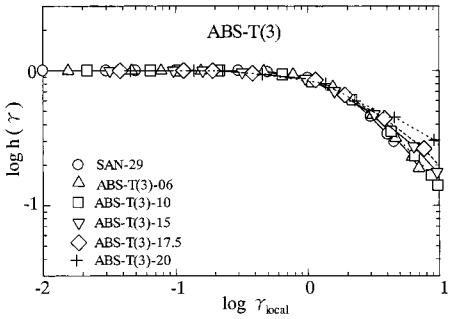

Figure 10. Plot of $h(\gamma)$ of ABS-T(3) with various rubber contents against local strain γ_{local}.

(fillers). In Figure 10, the $h(\gamma)$ data of the SAN chains in ABS-T(3) are plotted against γ_{local} thus evaluated. The plots for various w_r (various ϕ) excellently agree with each other and coincide with the $h(\gamma)$ vs γ plots for the pure matrix SAN-29. This result confirms the above expectation, demonstrating that the significant damping of the SAN chains in ABS-T(3) results from the usual mechanism (chain shrinkage faster than rotation) under the filler effect.

Damping Function of ABS-T(1). The rubber particles form the agglomerated networks in the ABS-T(1). In Figure 11, the $h(\gamma)$ data of the SAN chains in this ABS-T(1) and of the pure matrix SAN-29 are plotted against the externally applied strain γ. Clearly, $h(\gamma)$ of the SAN chains in this ABS changes only moderately with w_r and is close to $h(\gamma)$ of pure SAN-29. Consequently, the $h(\gamma)$ of the SAN chains is much less dependent on γ in ABS-T(1) than in ABS-T(3); cf. Figures 9 and 11.

This γ dependence in ABS-T(1) can be related to the agglomerated network structure therein: A majority of the matrix SAN chains in ABS-T(1) exists in large *pockets* in the network; see Figure 2. The local strain γ_{local} in the pockets (containing no rubber particles) should be close to the applied γ so that the filler effect is minor for the majority of the SAN chains therein. This

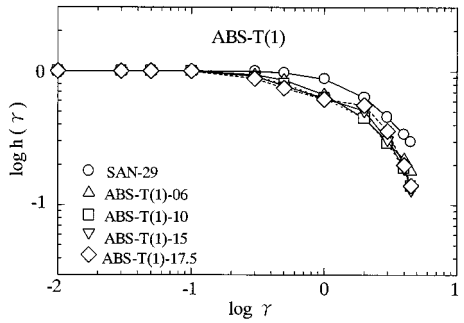

Figure 11. Damping functions $h(\gamma)$ of ABS-T(1) having different rubber content.

lack of the filler effect quite possibly leads to the approximate coincidence of $h(\gamma)$ of the SAN chains in ABS-T(1) and the pure matrix SAN-29 chains seen in Figure 11. In other words, the difference between $h(\gamma)$'s in ABS-T(1) and ABS-T(3) can be related to a difference in the magnitude of the filler effect for the majority of the SAN chains.

Conclusions

The time-strain separability was found for the SAN chains in two different types of ABS polymers. In the ABS polymer containing randomly dispersed rubber particles, the damping function $h(\gamma)$ of the SAN chains was more strongly dependent on γ than $h(\gamma)$ of the pure matrix SAN chains. This result quite possibly reflects the filler effect in that ABS polymer. In contrast, in the ABS polymers containing networks of the agglomerated rubber particles, the SAN chains exhibited less γ-dependent $h(\gamma)$ that was close to $h(\gamma)$ of the pure matrix chains. This behavior is attributable to lack of the filler effect in large pockets formed in this network.

References and Notes

(1) Aoki, Y. *J. Soc. Rheol. Jpn.* **1979**, *7*, 20.
(2) Aoki, Y. *J. Rheol.* **1981**, *25*, 351.
(3) Aoki, Y.; Nakayama, K. *J. Soc. Rheol. Jpn.* **1981**, *9*, 39.
(4) Aoki, Y.; Nakayama, K. *Polym. J.* **1982**, *14*, 951.
(5) Masuda, T.; Nakajima, A.; Kitamura, M.; Aoki, Y.; Yamauchi, N.; Yoshioka, A. *Pure Appl. Chem.* **1984**, *56*, 1457.
(6) Aoki, Y. *J Non-Newt. Fluid Mech.* **1986**, *2*, 91.
(7) Aoki, Y. *Macromolecules* **1987**, *20*, 2208.
(8) Hasegawa, R.; Aoki, Y.; Doi, M. *Macromolecules* **1996**, *29*, 6656.
(9) Osaki, K. *Rheol. Acta* **1993**, *32*, 429.
(10) Bernstein, B.; Kearsley, E. A.; Zapas, L. J. *Trans. Soc. Rheol.* **1963**, *7*, 391.
(11) Takahashi, M.; Li, L.; Masuda, T. *J. Rheol.* **1989**, *33*, 709.
(12) Ferry, J. D. *Viscoelastic Properties of Polymers*, 3rd ed.; Wiley: New York, 1980.
(13) Watanabe, H.; Sato, T.; Osaki, K.; Yao, M.-L. *Macromolecules* **1996**, *29*, 3890.
(14) Takahashi, M.; Urakawa, O.; Ebrahimi, N. G.; Isaki, T.; Masuda, T. *J. Soc. Rheol. Jpn.* **1996**, *24*, 37.
(15) Doi, M.; Edwards, S. F. *The Theory of Polymer Dynamics*; Clarendon: Oxford, 1986.
(16) Guth, E.; Gold, O. *Phys. Rev.* **1938**, *53*, 322.

MA002076L